

Localized Low-Frequency Vibrational Modes in a Simple Model Glass

Brian B. Laird and H. R. Schober

*Institut für Festkörperforschung, Forschungszentrum Jülich GmbH,
Postfach 1913, D-5170 Jülich 1, Federal Republic of Germany*

(Received 15 August 1990)

We examine the vibrational spectrum of a glass of soft spheres produced by quenching an equilibrated liquid (produced via constant-energy molecular-dynamics simulation) to zero temperature. Normal-mode analysis shows clearly the existence of (quasi)localized modes at the low-frequency end of the vibrational spectrum. The modes are found to be localized around atoms whose neighborhood structure differs significantly from the average glass environment. The effective masses of these modes range upwards from 10 atomic masses.

PACS numbers: 63.50.+x, 61.42.+h

At temperatures below 1 K, the properties of glasses differ strongly from those of crystals of the same material. This difference can be described well in terms of two-level states by the now standard tunneling model.^{1,2} However, in order to account for the anomalous behavior of the same glassy materials at temperatures between 1 and 10 K, where one finds additional states coexisting with the sound waves,³ this model must be extended. Recent neutron-scattering experiments have shown these additional states to be soft harmonic vibrations, localized to about 10 or more atoms.⁴ It is plausible to assume that both the two-level states and these soft harmonic vibrations have a similar structural origin.

A theory exploiting this idea was developed by Karpov, Klinger, and Ignat'ev.⁵ They describe both the two-level systems and the harmonic vibrational states by soft anharmonic potentials for some effective (reactive) coordinate. Fitting this model to the experimental data for various glasses gives between 20 and 70 for the number of atoms participating in the vibration.⁶ Even though such models give a consistent interpretation of the low-temperature experimental data, they do not give an answer to the question as to the physical nature of these tunneling or vibrating modes—neither can present experimental techniques. A microscopic understanding of these soft modes could give some important clues as to the physics of the glass transition.

In this paper, we present results of computer simulations that clearly show the existence of localized low-frequency vibrational modes in a simple soft-sphere glass. The approach is similar to the study of Nagel, Rahman, and Grest⁷ of vibrational localization in a modified Lennard-Jones glass, except that they concerned themselves only with the high-frequency modes. Low-frequency localized vibrations were found in a computer-generated model for amorphous silicon by Biswas *et al.*,⁸ but interpretation of the results is complicated by their use of a different potential to calculate the vibrational properties than was used to create the glass structure.

The idea of disorder-induced localization of excitations is most familiar from studies on electronic systems.⁹ Here, as the disorder is increased, the states at both the high- and low-energy ends of the density of states become localized first, while those in the center remain extended. For the case of phonons, however, true localization in a disordered system occurs only for those states at the high-frequency end of the normal-mode distribution,¹⁰ because in any elastic medium there are always extended acoustic modes at low frequency. Any low-frequency localized mode would then hybridize with these, destroying the strict local nature of the vibration. However, these hybrid modes retain their localized character, e.g., with regard to scattering properties. Such states are termed resonant or *quasilocalized*. These low-frequency quasilocalized modes are very important for the low-temperature properties.

The concepts of “localized” and “(quasi)localized” vibrations are well known in the phonon theory of defects in crystals.¹¹ The former denotes a vibration with a frequency outside the continuum of lattice frequencies. Such a vibration cannot couple to the lattice modes and its eigenvector decays exponentially with distance. These modes commonly occur either for very light impurities or for defects that cause large lattice strains such as self-interstitial atoms. In a glass, this type of vibration will be found in the high-frequency tail of the normal-mode spectrum. For low frequencies within the lattice continuum, where the host density of states is very low, resonant defect vibrations are possible. Such resonant modes are similar to localized modes in the usual definition and are often referred to as quasilocalized low-frequency modes. Like true localized vibrations, the eigenvector of such a mode is also localized to the defect and a few neighbors, but generally not as strongly, and does not decay exponentially.¹² Evidence for the existence of such resonant modes for self-interstitials in fcc metals was found at low frequencies by Dederichs, Lehmann, and Scholz,¹³ in addition to the usual high-frequency localized modes.

The amount of localization can be quantified in terms of the normalized eigenvectors e_a^m of the vibrational states, where the index m runs over all atoms in the sample and a labels the Cartesian coordinate. The motion of the mode is described by

$$u_a^m(t) = f(t)e_a^m/M_m^{1/2}, \quad (1)$$

where M_m is the mass of atom m and $u_a^m(t)$ is its displacement. Without loss of generality, we assume atom 1 to have the largest displacement. Within the harmonic approximation, the kinetic energy of the mode is then

$$\begin{aligned} E_{\text{kin}} &= \frac{1}{2} \sum_{m,a} M_m [\dot{u}_a^m(t)]^2 = \frac{1}{2} [\dot{f}(t)]^2 \\ &= \frac{1}{2} \sum_a M_{\text{eff}} (\dot{u}_a^1)^2, \end{aligned} \quad (2)$$

where the effective mass M_{eff} is defined as

$$M_{\text{eff}} \equiv M_1 / \sum_a (e_a^1)^2. \quad (3)$$

(Note that this definition of the effective mass is valid for not-too-large systems, but requires slight modification in the infinite-system limit.¹²) For localized and quasilocalized modes, M_{eff} is small and system-size independent, whereas for extended modes, it scales with the number of particles.

An alternative definition of localization often used is the participation ratio

$$p = \left\{ N \sum_m \left[\sum_a (e_a^m e_a^m)^2 \right] \right\}^{-1}. \quad (4)$$

For extended modes, p is of order unity. For localized or quasilocalized modes, it will scale inversely with the system size.

The two definitions can be mapped exactly into each other in only two extreme cases: $M_{\text{eff}} = M_1 \rightarrow p = 1/N$ and $M_{\text{eff}} = NM_1 \rightarrow p = 1$. For the interesting intermediate cases, only approximate correspondences hold. For self-interstitials in fcc metals, one finds for the low-frequency localized modes that $M_{\text{eff}} \approx 4$ or 5 times M_1 and for the high-frequency ones about half that value. The effective mass is sensitive to the defect-defect interaction—two interstitials clustered together will raise M_{eff} about a factor of 2. The effective mass for tunneling transitions of these defects was found to be similar to the one for the low-frequency modes.¹⁴

In a glass with its large distortions, we expect to find both types of localized vibrational modes. One cannot expect to find isolated defectlike structures, but there will always be strong interaction between such centers. Correspondingly, we expect the single-defect effective masses to be something like a lower limit of the ones in glasses.

To test these ideas, we perform a computer simulation for a system of soft spheres interacting with an inverse

sixth-power potential

$$u(r) = \epsilon(\sigma/r)^6. \quad (5)$$

To simplify the computer simulation and normal-mode analysis, the potential was cut off at $r/\sigma = 3.0$, and then shifted by a polynomial, $Ar^4 + B$, where A and B were chosen so that the potential and the force are zero at the cutoff. The inverse sixth-power potential was selected because this model material possesses, in its bcc crystal form, very soft shear modes,¹⁵ and it was hoped that this property would be reflected in a higher concentration of low-frequency resonant modes in the glass. As evidence of the universality of the phenomena discussed here, we also found low-frequency resonant modes in one- and two-component Lennard-Jones systems, but at such a low concentration that the collection of reasonable statistics would have been very difficult.

We produce our glass configurations by quenching a well-equilibrated liquid configuration of 500 soft spheres (1024 for the larger system) produced via constant-energy molecular-dynamics (MD) simulation with cubic periodic boundary conditions at a density $\rho\sigma^3 = 1.0$ and temperature $kT/\epsilon \approx 0.54$. This temperature is about 2.5 times the melting temperature at this density.¹⁶ The liquid is first quenched within the MD simulation by velocity rescaling to a reduced temperature of about 0.04, less than half the glass transition temperature, which for this density is about 0.09 (based on a preliminary examination of the diffusion constant). The system is then quenched to zero temperature using a combination steepest-descent-conjugate-gradient algorithm. In all, thirty different 500-atom configurations and three 1024-atom glass configurations were created in this way and analyzed.

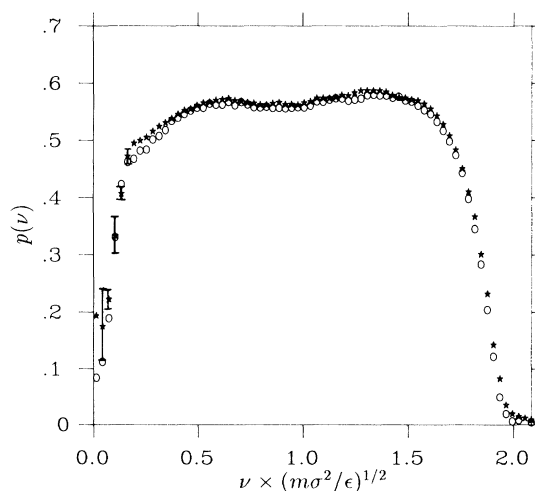


FIG. 1. The configurationally averaged participation ratio plotted as a function of frequency for both the 500-atom (stars) and 1024-atom (circles) systems.

For each glass configuration the force-constant matrix (using periodic boundary conditions) was calculated and diagonalized to yield the $3N$ ($N=500$ or 1024) normal-mode frequencies and eigenvectors. The participation ratio and effective mass for each mode were then calculated. These quantities were sorted by frequency into bins of width 0.03 and averaged over all configurations to yield a frequency profile. For the participation ratio, this frequency profile is plotted in Fig. 1 for both the 500- and 1024-atom configuration sets. The error bars were calculated by dividing the configurations into six sets of five and calculating $\langle p(\nu) \rangle$ for each and the standard deviation in the remaining six averages. Despite this coarse graining, this error estimate is still influenced by the inherent scatter in $p(\nu)$ and represents only a conservative upper bound of the actual statistical error. Except for a change in scale, the same plot for the effective mass is nearly identical. The most obvious feature of this plot is the dramatic drop of the participation ratio at both the high- and low-frequency ends of the spectrum. The drop at the high end of the spectrum is due to the usual high-frequency localized modes. We argue that the low participation ratios at the low-frequency end of the plot are due to the presence of resonant or quasilocalized modes. One indicator of the localized nature of these modes is that, for the very lowest frequencies, the participation ratios for the 1024-atom system are about a factor of 2 smaller than those for the 500-atom system, as is expected from Eq. (4).

In Fig. 2, we plot the configurationally averaged density of states for this system along with the same quantity with all modes (48 in all) subtracted out for which $p_c \leq 0.25$ (out of the thirty configurations only three contained no such modes). This cutoff was arbitrarily

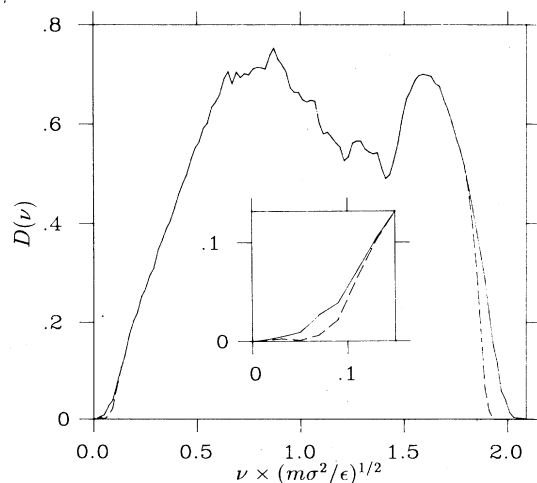


FIG. 2. The configurationally averaged vibrational density of states as a function of frequency for all modes (solid line) and all modes ($N=500$) with $p > 0.25$ (dashed line). Inset: An enlargement of the low-frequency tail of these curves.

chosen to yield a clear distinction between localized and nonlocalized modes; however, we have checked that the qualitative features of our result do not change for cutoffs in the range $0.15 \leq p_c \leq 0.35$. For $N=500$, $p_c=0.25$ corresponds roughly to $M_{\text{eff}}=25$. One sees that these resonant modes make a significant contribution to the density of states at very low frequencies, and, thus, would be expected to profoundly affect the low-temperature behavior of the glass.

Some insight into the structural nature of these resonant modes can be obtained by examining the two-particle radial distribution function $g(r)$. In Fig. 3, we plot this function calculated by averaging over all available zero-temperature glass configurations. Also, for each low-frequency resonant mode ($p_c \leq 0.25$), the particle with the largest displacement was determined, and $g(r)$ calculated using this particle as the central atom. Averaged over all the resonant modes, this quantity is also plotted in Fig. 3. [The error bars were calculated as for $p(\nu)$.] From these plots, we can see that the nearest-neighbor shell is more compressed and less dense for the resonant-mode central atom than that for the average particle. This first-shell particle deficiency in the resonant $g(r)$ is made up for by a small peak just outside the first peak, after which the integrated particle number (see the inset to Fig. 3) for the two displayed distribution functions are nearly identical. The qualitative nature of this difference is relatively insensitive to the exact value of p_c ($0.15 \leq p_c \leq 0.35$) and is, therefore, a real effect—not just a statistical fluctuation. Thus, the existence of these modes cannot be derived from the average structural properties of the glass, as is

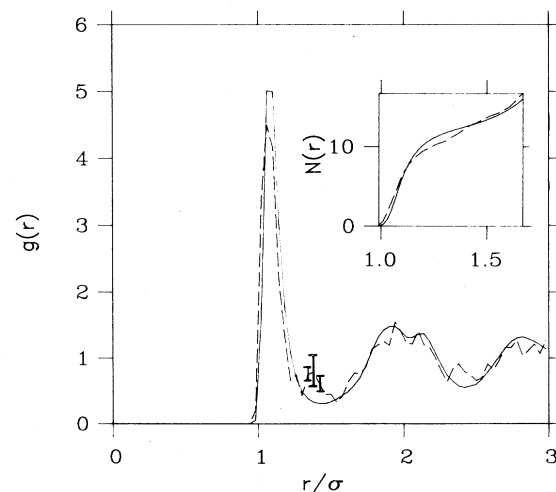


FIG. 3. The configurationally averaged two-particle radial distribution function $g(r)$ measured for the full system (solid line) and using as the central atom only those particles with the largest displacement for some mode ($N=500$) with $p < 0.25$ (dashed line). Inset: The integrated form of this quantity—the total radial particle number $N(r)$.

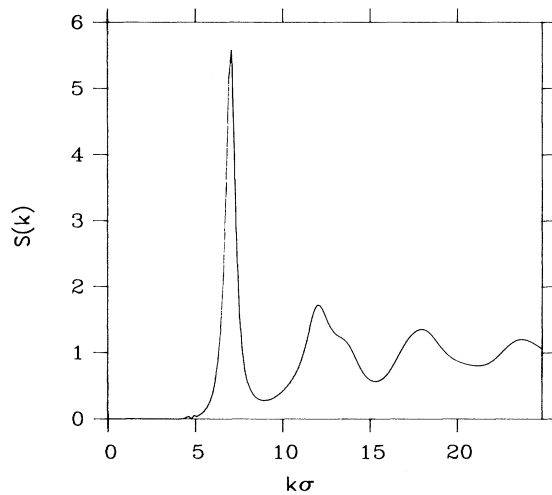


FIG. 4. The configurationally averaged structure factor for our inverse sixth-power glass at zero temperature.

done, for example, in the effective-medium approximation.¹⁷

To illustrate the glassy nature of our zero-temperature sample and to aid comparison of this model glass to real materials, we have also plotted (Fig. 4) the configurationally averaged structure factor $S(k)$ for our system. This function was obtained by Fourier transforming the $g(r)$ using a method due to Verlet¹⁸ to correct errors due to truncation of $g(r)$.

Our investigation shows clearly the existence of localized low-frequency modes in accordance with recent experiments and theoretical conjectures. These low-frequency modes are found in much lower concentrations (10^{-3}) than their high-frequency counterparts. As is to be expected, their localization is also much weaker. The most localized modes are found to have effective masses of about 10 to 30 atomic masses. The frequencies of these modes are well below $\frac{1}{10}$ th of the maximum vibrational frequency. The two-particle radial distribution function $g(r)$ for those atoms that maximally contribute to the low-frequency localized modes indicates a structural difference from that of the average glass: The nearest-neighbor distance is reduced and about one atom is pushed from the nearest-neighbor shell into the region

where the average $g(r)$ has its first minimum. A more detailed analysis of the structural origin of these modes is under way.

We are grateful for many stimulating discussions with U. Buchenau. This material is based on work supported by the North Atlantic Treaty Organization under a grant awarded to B.L.

¹P. W. Anderson, B. I. Halperin, and C. M. Varma, *Philos. Mag.* **25**, 1 (1972).

²W. A. Phillips, *J. Low Temp. Phys.* **7**, 351 (1972).

³S. Hunklinger and A. K. Raychoudhuri, *Prog. Low Temp. Phys.* **9**, 267 (1986).

⁴U. Buchenau, H. M. Zhou, N. Nücker, K. S. Gilroy, and W. A. Phillips, *Phys. Rev. Lett.* **60**, 1368 (1988).

⁵V. G. Karpov, M. I. Klinger, and F. N. Ignat'ev, *Zh. Eksp. Teor. Fiz.* **84**, 760 (1983) [*Sov. Phys. JETP* **57**, 439 (1983)].

⁶U. Buchenau, Yu. Galperin, V. Gurevich, and H. R. Schober (to be published).

⁷S. R. Nagel, A. Rahman, and G. S. Grest, *Phys. Rev. Lett.* **53**, 368 (1984).

⁸R. Biswas, A. M. Bouchard, W. A. Kamitakahara, G. S. Grest, and C. M. Soukoulis, *Phys. Rev. Lett.* **60**, 2280 (1988).

⁹D. J. Thouless, in *Ill-Condensed Matter*, edited by R. Balian, R. Maynard, and G. Toulouse (North-Holland, Amsterdam, 1979).

¹⁰S. John, H. Sompolinski, and M. J. Stephen, *Phys. Rev. B* **27**, 5592 (1983).

¹¹A. A. Maradudin, E. W. Montroll, G. H. Weiss, and I. P. Ipatova, *Theory of Lattice Dynamics in the Harmonic Approximation*, Solid State Physics Suppl. 3 (Academic, New York, 1971).

¹²P. H. Dederichs and R. Zeller, in *Point Defects in Metals II*, Springer Tracts in Modern Physics Vol. 87 (Springer-Verlag, Berlin, 1980).

¹³P. H. Dederichs, C. Lehmann, and A. Scholz, *Phys. Rev. Lett.* **31**, 1130 (1973).

¹⁴H. R. Schober and A. M. Stoneham, *Phys. Rev. B* **26**, 1819 (1982).

¹⁵W. G. Hoover, S. G. Gray, and K. W. Johnson, *J. Chem. Phys.* **55**, 1128 (1971).

¹⁶W. G. Hoover, D. A. Young, and R. Grover, *J. Chem. Phys.* **56**, 2207 (1972).

¹⁷W. Schirmacher and M. Wagener, in *Dynamics of Disordered Materials*, edited by D. Richter, A. J. Dianoux, W. Petry, and J. Teixeira (Springer-Verlag, Berlin, 1980).

¹⁸L. Verlet, *Phys. Rev.* **165**, 201 (1968).